Screening of Potential Compounds in Tomato (*Solanum lycopersicum*) as Candidates for Anti Diabetes Mellitus Complications

Sekararum Narwasthu[1,2], Muhamad Fahmi[3], Nia Kurnianingsih[4], Titin Andri Wihastuti[5], and Fatchiyah Fatchiyah[1,2*]

[1]*Department of Biology, Faculty of Mathematics and Natural Sciences, Universitas Brawijaya, Jl. Veteran 10-11, Malang 65145, Indonesia*

[2]*Research Center of Smart Molecule of Natural Genetics Resources, Universitas Brawijaya, Jl. Veteran 10-11, Malang 65145, Indonesia*

[3]*Research Department, Research Institute for Humanity and Nature, 457-4 Motoyama, Kamigamo, Kita-ku, Kyoto 6038047, Japan*

[4]*Department of Physiology, Faculty of Medicine, Universitas Brawijaya, Jl. Veteran 10-11, Malang 65145, Indonesia*

[5]*Department of Basic Nursing Science, Medical Faculty, Universitas Brawijaya, Jl. Puncak Dieng, Malang 65151, Indonesia*

Corresponding author:

tel: +62-341-575-841
email: fatchiya@ub.ac.id

Received: January 24, 2024
Accepted: April 2, 2024

DOI: 10.22146/ijc.93505

Abstract: *This study aimed to identify the potential of natural compounds in tomatoes for diabetic complications intervention using amino acid profile, HP-TLC, antioxidant assay, enzymatic inhibitor assay, and* in silico *approach. Fresh air-dried tomatoes were analyzed for several screening assays including amino acid determination, HP-TLC, antioxidant activity using FRAP, α-amylase, and α-glucosidase enzyme inhibition. Virtual screening, molecular docking and molecular dynamics were performed using Molinspiration, pKcSM, AutoDock Vina, Discovery Studio, PyMOL, and Yasara software. Tomato bioactive compounds showed promising drug-likeness, antioxidant and α-amylase/glucosidase inhibitory activities, and potential for AGE-RAGE interaction. Out of 19 compounds from whole tomatoes complying with Lipinski's rule of five, genistein, apigenin, and naringenin exhibited high oral absorption potential. Tomato contains genistein compound based on HP-TLC and the compound has high antioxidant and antidiabetic activities. Genistein has a stronger binding affinity with RAGE compared to AGE, indicating its potential as a competitive inhibitor. Additionally, genistein displayed stable ligand movements and higher binding energy values in MD simulations compared to the control. These findings suggest the potential of tomato bioactive compounds for further development as antidiabetic agents targeting AGE-RAGE interaction. In conclusion, genistein in tomatoes is indicated as a candidate for anti-complications of diabetes mellitus.*

Keywords: *AGEs; diabetes; genistein; RAGE; tomatoes*

■ INTRODUCTION

Diabetes mellitus (DM) is a chronic condition caused by insufficient insulin hormone production and function as blood glucose regulation, thus generating chronic hyperglycemia [1]. The prevalence of DM is increasing worldwide and positioned as the fifth leading cause of mortality and morbidity. In the global population, Indonesia ranked 5th for individuals aged 20–79 with DM in 2021 [2]. The current basic health research in Indonesia revealed a significant increase in diabetes prevalence from 6.9% in 2013 to 8.5% in 2018 [3]. DM has two types of disease namely type 1 and type 2. Type 1 DM is characterized by insufficient insulin release by pancreas. Type 2 DM is characterized by insulin resistance, thus leading to hyperinsulinemia. Both conditions provoke a hyperglycemia state and failure of glucose utilization for energy expenditures [4].

Among both types of DM, type 2 DM (T2DM) is the

most common in the population. The T2DM is identified in more than 90% of cases of DM and is the 5th leading cause of death in individuals aged 50–74 [5]. Prolonged hyperglycemia in DM causes systemic organ complications involving the role of pro-inflammatory biomarkers called advanced glycation end products (AGEs) and its receptors, receptor for advanced glycation end products (RAGE) [6]. The AGEs are produced through non-enzymatic glycation of proteins and glucose. Different AGEs can be found in human blood, tissue, and processed food [7]. AGEs pose a significant health risk, damaging organs like kidneys, retinas, and bones. Their toxic effect on pancreatic beta cells further fuels diseases like diabetes and heart disease. Understanding these risks and implementing strategies to lower AGE exposure is crucial for long-term health [8-9].

There are drugs to inhibit AGEs, but they have severe side effects. Aminoguanidine, OPB-9195, and pyridoxamine are examples of AGE inhibitor drugs that have been clinically tested, but all have significant side effects that can cause infection, liver dysfunction, and lupus-like symptoms. Therefore, an alternative is needed, which is to use plants as natural AGE inhibitors. Plants have various compounds that can inhibit AGEs, such as antioxidants, metal chelators, and carbonyl sorbents. Several studies have shown that plants can inhibit AGEs without causing severe side effects [10].

In one study, bioactive compounds of Bajakah (*Spatholobus suberectus*) demonstrated a significant potential to prevent the formation of AGEs and oxidative stress seen in T2DM due to its antioxidant content and antiglycative properties. Furthermore, tomatoes also possess high antioxidant effects and are readily available [11]. Building on these findings, this study will explore whether bioactive compounds present in fruits, specifically tomatoes, are capable of acting as effective AGEs inhibitors. Additionally, the study aims to identify the bioactive compounds within tomatoes that hold the greatest potential for antidiabetic complications.

■ EXPERIMENTAL SECTION

Materials

The research materials used were purchased from Sigma-Aldrich: genistein (cat. no. G6776), methanol, sodium hydroxide, potassium ferricyanide, trichloroacetic acid, 4-nitrophenyl-α-D-glucopyranoside, iron(III) chloride, starch, and α-glucosidase from *Saccharomyces cerevisiae*. The following materials were obtained from TCI: α-amylase diluted with starch from *Bacillus amyloliquefaciens*, and ascorbic acid. Three varieties of *Solanum lycopersicum* from three sub-districts in Malang, Indonesia, were used in this research. They were Sirvo tomatoes from Tumpang, Marvel tomatoes from Karangploso, and Montana tomatoes from Batu, East Java, Indonesia.

Instrumentation

The instruments used in this study were a shaker water bath (Memmert), rotary evaporator (IKA HB 10), UV-vis spectrophotometer (SmartSpec Plus™, BioRad Laboratories Inc., Hercules, CA, USA), and set instrument high-performance thin-layer chromatography-CAMAG (Linomat 5, TLC Scanner 4, dan UV Cabinet 4).

Procedure

Physicochemical, pharmacokinetic, and toxicity screening

A list of 42 natural compounds found in tomatoes was compiled from a study by Kumar et al. [12]. We evaluated the drug-likeness of these compounds using the Molinspiration website (https://www.molinspiration.com/) following Lipinski's rule of five, including molecular weight (< 500), log P (< 5), hydrogen bond acceptor (< 10), and hydrogen bond donors (< 5) [13]. The pharmacokinetics and toxicity properties of compounds were analyzed using pKcSM (https://biosig.lab.uq.edu.au/pkcsm/prediction) [14]. This subsequent stage of screening resulted in the selection of five final compounds.

Plant extraction tomato sample preparation

Tomato preparation begins with the tomato fruit being washed, weighed, and cut into several parts. Tomatoes are dried in an oven at 50 °C. The dried tomato samples were pulverized so that they became tomato powder simplicia [15]. A total of 5.0 g of tomato simplicia was extracted with a ratio of methanol and distilled water (90:10, v/v) at 80 °C for 1 h in a water

bath, then filtered and evaporated using a rotary evaporator [16].

Amino acid determination

Characterization of essential and non-essential amino acid profiles was conducted in PT. Saraswanti Indo Genetech, Bogor, West Java, Indonesia using the ultra performance liquid chromatography (UPLC) method, 18-5-17/MU/SMM-SIG (UPLC-PDA) for the amino acids L-alanine, glycine, L-isoleucine, L-leucine, L-serine and L-tyrosine test, and 18-5-63/MU/SMM-SIG (HPLC-PDA) for the amino acid L-tryptophan test. The UPLC used column AccQ.Tag Ultra C18 1.7 μm (2.1 × 100 mm). A photodiode array (PDA) detector, calibrated to a wavelength of 260 nm, was used for detection. The mobile phase consisted of a gradient system comprised of A) eluent A concentrate Amino Acid Analysis AccQ.Tag Ultra, B) eluent B Amino Acid Analysis AccQ.Tag Ultra diluted to 10% in water, C) aquabidest, and D) eluent B Amino Acid Analysis AccQ.Tag Ultra. The flow rate was maintained at a constant rate of 0.5 mL/min [17].

High-performance thin-layer chromatography

This analysis was performed using a set of HP-TLC-CAMAG instruments consisting of Linomat 5, TLC Scanner 4, and UV Cabinet 4. Three tomato samples and standards were diluted in methanol. The solution was spotted on the silica gel plate F_{254}. Next, the silica gel plate F_{254} was eluted in a mobile phase with toluene-acetate ethyl-formic acid eluent. The spots were observed under UV chamber of 254 and 366 nm, and a TLC scanner. Standard curves were prepared by varying the injection volume from 1.0, 1.5, 2.0, 2.5, 3.0, and 3.5 μL. Each solution was injected with a volume of 10 μL of genistein standard solution [18].

Antioxidant activity test with ferric reducing antioxidant power (FRAP) method

Samples were diluted with 0.1% HCl in methanol at concentrations of 0, 1, 2, 4, 6, 8, and 10 μg/mL. Gold standard solutions of genistein was prepared at concentrations of 0, 1, 2, 4, 6, 8, and 10 μg/mL. The solution was mixed with 200 mmol/L phosphate buffer pH 6.6 of 2.5 mL and 1% potassium ferricyanide of 2.5 mL. The solution was incubated at 50 °C for 30 min, and 2.5 mL of 10% TCA was added and homogenized. Then, 5 mL of solution was taken and transferred to a new test tube. The solution was added with 5 mL of distilled water and 1 mL of 0.1% ferric chloride, and the absorbance was measured at 700 nm using UV-vis spectrophotometry [19]. Antioxidant activity was calculated by the Eq. (1). The IC_{50} value was determined by creating a linear regression equation with the sample concentration and its percentage antioxidant activity on the x and y axes, respectively.

$$\%\text{Antioxidant} = \left(\frac{\text{Control}_{\text{abs.}} - \text{Sample}_{\text{abs.}}}{\text{Control}_{\text{abs.}}} \right) \times 100\% \qquad (1)$$

Enzyme inhibition assay of α-amylase and α-glucosidase

In the α-amylase enzyme inhibition assay, acarbose standard and extracts with a range of concentration variations were added as much as 250 μL into a test tube. The extract was mixed with 250 μL of α-amylase enzyme and incubated for 20 min at 37 °C. After incubation, 1% amylum was added and incubated for 10 min. DNS was added as 500 μL, and the sample was heated for 5 min. The absorbance was measured at 490 nm [20].

In the enzyme inhibition assay of α-glucosidase, 50 μL of plant extracts with varying concentrations from 12.5 to 400 μg/mL were incubated with 10 μL of α-glucosidase for 20 min at 37 °C with the addition of 125 μL of 0.1 M phosphate buffer (pH 6.8). After 20 min, 4-nitrophenyl-β-D-glucopyranosiduronic acid substrate was added and incubated for 30 min. The reaction was stopped by the addition of 0.1 N Na_2CO_3 (50 μL), and the final absorbance was measured at 405 nm [21]. Calculation of percentage of inhibition uses the following Eq. (2).

$$\%\text{Inhibition} = \left(\frac{\text{Control}_{\text{abs.}} - \text{Sample}_{\text{abs.}}}{\text{Control}_{\text{abs.}}} \right) \times 100\% \qquad (2)$$

In silico analysis

Data mining. The five compounds that successfully passed the previously described screening stage were selected as the ligands for molecular docking. As control ligands, we included two AGEs, namely argpyrimidine and pentosidine. The three-dimensional structure of the ligands was retrieved from the PubChem database

(https://pubchem.ncbi.nlm.nih.gov/). For our investigation into T2DM intervention, we designed RAGE as the target protein. The structure of RAGE was downloaded from the RCSB Protein Data Bank with PDB ID: 2M1K (https://www.rcsb.org/) [6,22].

Molecular docking and visualization. The 3D structure of the protein was prepared using the Biovia Discovery Studio 2019 software, which involved removing any attached native ligands and water molecules. Meanwhile, the ligands were prepared using Open Babel, integrated with PyRx 8.0 software, for energy minimization [23]. Prior to the docking study, the docking parameters and algorithm were validated by re-docking the native ligand to the target receptor [24]. Protein-ligand docking was simulated using AutoDock Vina in PyRx software [25]. Ligand binding poses were combined using PyMOL and analyzed for residue interactions using Biovia Discovery Studio. Complexes with binding energies lower or equal to AGEs were considered for downstream analysis [26-27].

Molecular dynamics. Molecular dynamics is performed using Yasara software. The parameters of the simulation included pH 7.4, salt content (NaCl) of 0.9%, a temperature of 37 °C, pressure 1 atm, and simulation time of 20 ns [28].

■ RESULTS AND DISCUSSION

Physicochemical, Pharmacokinetic, and Toxicity Potencies of Tomato Compounds

The drug-likeness prediction was performed as an initial stage for drug development by following Lipinski's rule of five [29]. The results showed that 19 compounds successfully passed this selection stage (Table S1). A portion of 5 compounds in tomatoes met Lipinski's rule of five (Table 1A) determined using the following characteristics involving molecular weight < 500 kDa, hydrogen bond donor < 5, hydrogen bond acceptor < 10, and a log P value < 5. A single minor violation of one of those parameters is tolerable. Compounds with a molecular weight > 500 Da typically indicate low permeability due to their large size, thus allowing them to be absorbed more slowly in the body. Therefore, the compounds are ineffectively crossing the cell membranes [30-31]. Hydrogen bond capacity is indicated by the number of hydrogen bond donors. Higher hydrogen bonding capacity relates to higher energy for

Table 1. Physicochemical, pharmacokinetic, and toxicity potencies of tomato compounds from (A) Molinspiration screening and (B) pKcSM screening

A. Molinspiration screening result of the bioactive compound in tomato

CID	Compound	Canonical SMILES	miLogP	TPSA	MW	nON	nOHNH	nViolate	nrotb
5280443	Apigenin	C1=CC(=CC=C1C2=CC(=O)C3=C(C=C(C=C3O2)O)O)O	2.46	90.89	270.24	5	3	0	1
5280961	Genistein	C1=CC(=CC=C1C2=COC3=CC(=CC(=C3C2=O)O)O)O	2.27	90.89	270.24	5	3	0	1
5280863	Kaempferol	C1=CC(=CC=C1C2=C(C(=O)C3=C(C=C(C=C3O2)O)O)O)O	2.17	111.12	286.24	6	4	0	1
932	Naringenin	C1C(OC2=CC(=CC(=C2C1=O)O)O)C3=CC=C(C=C3)O	2.12	86.99	272.26	5	3	0	1
4788	Phloretin	C1=CC(=CC=C1CCC(=O)C2=C(C=C(C=C2O)O)O)O	2.66	97.98	274.27	5	4	0	4

B. pKcSM screening result of the selected bioactive compound in tomato

CID	Compound	VDss	BBB permeability	CNS permeability	Hepatotoxicity	Skin Sensitization	CYP3A4 inhibitor	Intestinal absorption
5280443	Apigenin	0.822	−0.734	−2.061	No	No	No	93.25
5280961	Genistein	0.094	−0.710	−2.048	No	No	No	93.38
5280863	Kaempferol	1.274	−0.939	−2.228	No	No	No	74.29
932	Naringenin	−0.015	−0.578	−2.215	No	No	No	91.31
4788	Phloretin	0.765	−0.927	−2.535	No	No	No	60.50

the absorption process [32]. Log P suggests the balance of lipophilicity of the compounds. Log P value reflects the solubility of compounds in polar and non-polar solvents. A larger log P value correlates with the incline of hydrophobic characteristics [33]. Because the molecules in the lipid bilayer membrane are separated longer, they will be dispersed widely throughout the body, increasing the level of toxicity caused by overly hydrophobic compounds. This decreases the compound's selective ability to inhibit the target protein. As the log P number gets more negative, the molecule's ability to pass through membranes decreases [31].

To determine potential of oral drug candidates, the characteristics of pharmacokinetics are important to evaluate. The percentage of a compound absorbed in the human gut (%HIA) predicted by pKcSM software. The percentage > 80% indicates good intestinal absorption, and 30% indicates poor absorption [34]. Absorption analysis presented in Table 1B, demonstrates remarkable performance for genistein, apigenin, and naringenin as potential oral drug candidates as visualized by the percentage of absorption value. The parameter of volume of distribution at steady state (VDss) refers to drug distribution throughout the body after reaching steady state. High VDss means more drugs distributed to tissues than circulatory blood. VDss values can be categorized as less than −0.15 for low distribution and above 0.45 for high distribution. Drugs reaching the brain directly can cause fewer side effects, be less toxic, and work better. This ability is measured in animals as "log BB". Compounds with log BB > 0.3 easily penetrate to brain tissue, meanwhile score < −1 has difficulty to across the BBB [35].

BBB penetration, the study investigated the ability of drugs to reach the deeper central nervous system (CNS). A compound's log PS value > −2 suggests good CNS penetration, while a value < −3 indicates limited access. According to the pKCSM prediction, genistein and naringenin have log VDss ≥ −0.15, while kaempferol, apigenin, and phloretin have log VDss > 0.45 (Table 1B), meaning that they can be distributed moderately to yield higher concentrations in tissue than in plasma. Interestingly, all tomato compounds have a log BBB value ≥ −1, meaning that these compounds can readily cross the BBB and have log PS value > −3, which means that they can penetrate the CNS [36]. The liver enzyme CYP450 can deactivate certain drugs and inhibit other molecules, thus promoting drug interactions. Therefore, drug candidates need to be evaluated for their interactions with CYP450. The pKCSM software can predict these interactions for five key CYP isoforms. Based on the result below, none of these compounds were predicted to be CYP3A4 inhibitors [37].

We studied how different amino acids (AA) affect insulin sensitivity and release (Table 2). Glycine and serine from Marvel tomato can improve insulin sensitivity, while alanine, tyrosine, and isoleucine from Montana tomato can reduce it. Additionally, alanine, isoleucine, leucine, tryptophan, and valine from Montana tomato may inhibit insulin release. Noteworthy,

Table 2. Specific essential and non-essential of three tomato varieties to improve or reduce the insulin function associated with diabetes

Function	Amino acid		Sirvo tomato	Marvel tomato	Montana tomato
Improved insulin sensitivity	Non-Essential	Glycine	3608.27	3930.62	2710.51
		L-Serine	3441.62	3506.48	2460.08
Reduction of insulin sensitivity	Non-Essential	L-Alanine	3764.21	3527.03	3100.92
		L-Tyrosine	2122.77	2790.37	1440.65
	Essential	L-Isoleucine	1652.88	2293.80	1528.39
Reduction of insulin secretion	Non-Essential	L-Alanine	3764.21	3527.03	3100.92
	Essential	L-Isoleucine	1652.88	2293.80	1528.39
		L-Leucine	3516.31	4132.82	2656.93
		L-Tryptophan	1043.00	701.69	631.96
		L-Valine	1865.43	2477.72	1682.88

tryptophan and alanine seem to have a dual effect, reducing both sensitivity and release.

These findings are in line with previous studies by van Sloun et al. [38], which reported that glycine, serine, glutamine, and asparagine were associated with improved insulin sensitivity. At the same time, glutamate, tyrosine, isoleucine, and alanine influence decreasing insulin sensitivity. Moreover, this research also identified glutamate, tyrosine, isoleucine, and alanine as potent insulin sensitivity inhibitors. Interestingly, their work further linked phenylalanine and tyrosine to reduced insulin secretion and elevated glucose levels, supporting existing evidence that connects these AAs to insulin resistance and diabetes. This study further expands our understanding of tryptophan's role by demonstrating its potential to impede insulin secretion. This finding coincides with its predominant metabolic pathway (> 95%), the kynurenine pathway, which has been linked to inflammation, immune response, and excitatory neurotransmission. Previous research suggests that metabolites from this pathway could contribute to diabetes in humans by inhibiting both proinsulin synthesis and insulin release. Additionally, existing evidence indicates that elevated alanine levels may be linked to impaired insulin action in individuals with T2DM [38-39].

The TLC results show that the gold standard with several volume variations (1–3.5 µL) has an R_f value of 0.378, in Montana and Sirvo tomatoes, which also have the same R_f value, in contrast to Marvel tomatoes, which have an R_f value of 0.386 (Fig. 1). The range of values indicates the presence of genistein compounds in accordance with the gold standard. Another study using the same KLT method showed the results of genistein Rf values ranging from 0.38–0.39 derived from Semen Sojae Praeparatum (fermented *Glycine max* seeds) and *Glycine max* seeds [40].

Antioxidant and Antidiabetic Activity

The test of genistein compounds' activity as antioxidants was conducted by FRAP scavenging assay. The antioxidant test shows that Marvel tomato and Montana tomato have the highest antioxidant activity with

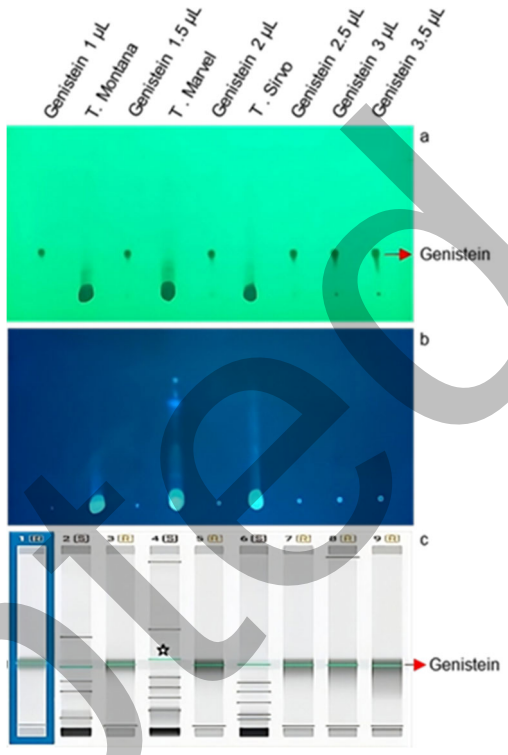

Fig 1. TLC chromatograms of the genistein compound of Montana, Marvel, and Sirvo tomatoes compared with genistein gold standard were documented at 254 nm (a), 366 nm (b), and TLC scanner (c), the star is R_f for genistein of Marvel tomato

IC_{50} of 7.76 and 7.94 µg/mL. In the antioxidant activity test, genistein as the gold standard with IC_{50} of 8.90 µg/mL, followed by ascorbate compound as control with IC_{50} of 9.30 µg/mL and Sirvo tomato with IC_{50} of 9.60 µg/mL (Fig. 2). Antioxidants are natural or synthetic compounds that scavenge free radicals, protecting cells and promoting overall health. They donate electrons to free radicals, stabilize them, and prevent their harmful effects. Montana and Marvel's tomatoes are likely rich in diverse antioxidants. By chelating metal ions like Cu^{2+} and Fe^{2+} and stabilizing unpaired electrons with its phenolic rings, bioactive compounds in tomatoes exhibit strong antioxidant properties [41].

Based on the results of the α-amylase enzyme inhibition test, it shows that Montana tomato has the greatest activity among other tomato samples with IC_{50} of 7.6 µg/mL. In comparison, Sirvo tomato has the lowest

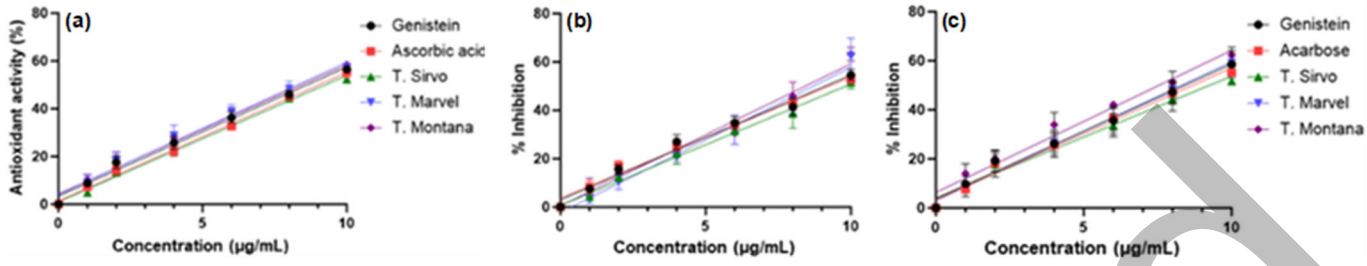

Fig 2. (a) Antioxidant activity by gold standard (genistein), ascorbic acid, Sirvo tomato, Marvel tomato and Montana tomato at various concentration, (b) inhibitory percentage of α-amylase enzyme, and (c) inhibitory percentage of α-glucosidase enzyme by gold standard (genistein), acarbose, Sirvo tomato, Marvel tomato and Montana tomato at various concentration

α-amylase inhibitory enzyme activity with IC_{50} of 9.52 µg/mL. In the α-amylase enzyme inhibition activity test, acarbose was used as a positive control. In the α-glucosidase enzyme inhibition activity test, acarbose with the same concentration variation was used for comparation. These results show that Montana tomato has the highest inhibitory activity with an IC_{50} value of 7.3 µg/mL (Fig. 2). Acarbose is a drug that works by inhibiting the enzyme that breaks down carbohydrates in the digestive tract [42]. In people with DM, high blood glucose levels can lead to serious complications. Inhibitors of carbohydrate-degrading enzymes such as amylase and glucosidase can help lower blood glucose levels by inhibiting the digestion of carbohydrates. This causes glucose to be released into the bloodstream slowly, thus controlling blood glucose levels [43].

Molecular Docking and Molecular Dynamics

Docking methods were used to predict the binding modes and affinities of proteins and target compounds. To achieve accurate docking results, it is critical to predict the position of the native ligand within the receptor binding site as well as understand the associated physicochemical molecular interactions [44]. The docking results of RAGE and argpyrimidine, RAGE and pentosidine, two AGEs, showed binding energy values of −5.6 and −5.7 kcal/mol, respectively. The bonds formed on RAGE, and argpyrimidine are hydrogen bonds at amino acid residues lys169, gly170, thr195, ala197 and hydrophobic bonds at amino acid residue pro204, while the bonds formed on RAGE and Pentosidine are hydrogen bonds at amino acid residues thr195, lys169, asp201 (Fig. S1 and Table S2).

Specifically, pentosidine interacts with domains C and V, while argpyrimidine connects upstream of the C1 domain of RAGE [45]. Interestingly, the five tomato compounds showed lower binding energy values compared to AGEs, with the lowest binding energy value being genistein at −7.3 kcal/mol. RAGE and apigenin formed hydrogen bonds indicated by amino acid residues leu49, gln67, val78, and gln67, while hydrophobic bonds at leu49, pro45, pro66, val78, and pro80. RAGE and genistein form hydrogen bonds indicated by amino acid residues lys169, gly170, thr195, and gly200, electrostatic bonds at asp201, and hydrophobic bonds at val194 and pro196. The bonds between RAGE and kaempferol are hydrogen bonds at ser74, gln67, and arg77. The bonds between RAGE and naringenin formed are hydrogen bonds at gln47, arg77, and gln67 and hydrophobic bonds at pro45, pro80, and pro87.

RAGE and phloretin formed hydrogen bonds at thr195 and hydrophobic bonds at lys169, pro196, and pro204. This suggests that these tomato compounds have a stronger bond with the target protein, specifically RAGE in this case. The binding energy value obtained from the docking results can determine the strength of the bond between the ligand and the RAGE target protein. Binding energy represents the strength of the interaction between two or more molecules, and a higher binding energy value indicates a lower affinity between the receptor and the ligand [46]. Apigenin, kaempferol, and naringenin interact with RAGE in the

V domain, while genistein and phloretin interact in the C1 domain (Fig. S1 and Table S2).

The V and C1 domains constitute structural and functional units, serving as the binding sites for most ligands [47]. To determine the interaction between AGEs and specific bioactive compounds, all of bioactive compounds of tomatoes fruit analyzed with argpyrimidine and pentosidine. The analysis result showed binding energy values respectively, argpyrimidine and genistein (40.1 kcal/mol), argpyrimidine and naringenin (29.3 kcal/mol), argpyrimidine and apigenin (20.1 kcal/mol), argpyrimidine and phloretin (17.0 kcal/mol), as well as argpyrimidine and kaempferol (10.2 kcal/mol). Similar with previous bioactive compound, pentosidine has the highest binding energy with genistein (50.0 kcal/mol), followed by pentosidine and naringenin (36.1 kcal/mol), pentosidine and kaempferol (32.8 kcal/mol), pentosidine and apigenin (30.4 kcal/mol), as well as pentosidine and phloretin (15.8 kcal/mol) (Fig. S2 and Table S3).

The docking results for RAGE-genistein-kaempferol showed the highest binding energy value of –6.0 kcal/mol and RAGE-apigenin-pentosidine of –5.8 kcal/mol (Fig. 3 and Table 3). Both hydrogen bonds and hydrophobic interactions suggest a highly specific and stable binding between complex RAGE-bioactive with AGEs. This strong interaction could potentially enhance the efficacy of these compounds in inhibiting AGE-mediated damage [48]. The bonds formed during the docking process include hydrogen bonds and hydrophobic bonds. In the docking of RAGE-naringenin-argpyrimidine, RAGE-kaempferol-argpyrimidine, and

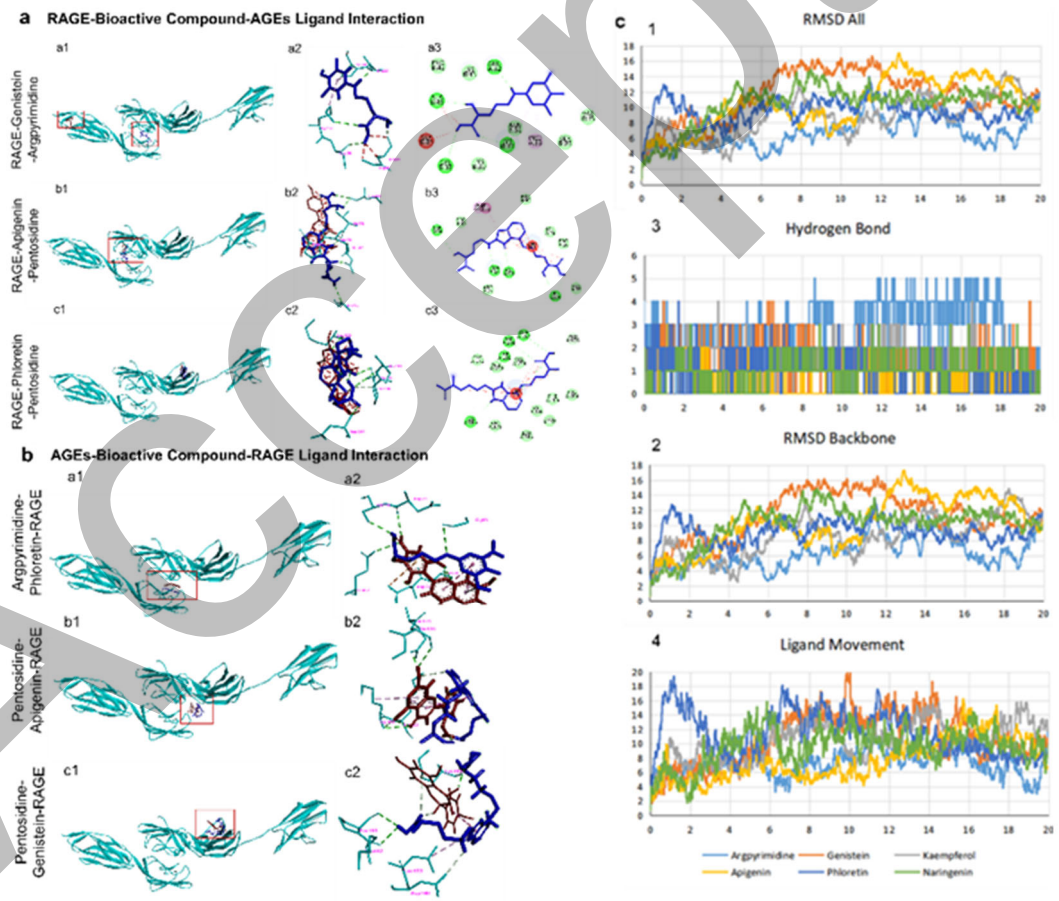

Fig 3. Comparation of binding poses and ligand interaction between complex RAGE-bioactive compound with (a) AGEs and complex AGEs-bioactive compound tomato fruit with (b) RAGE, and (c) structural stability and integrity of RAGE with selected compounds according to the (1) RMSD All, (2) hydrogen bond, (3) RMSD backbone, and (4) ligand movement

Table 3. Interaction table of complex RAGE-bioactive compound with AGEs (A) and complex AGEs-Bioactive compound tomato fruit with RAGE (B)

Point interaction	Chemistry bond	Type	Binding affinity (kcal/mol)
A. RAGE-bioactive compound-AGEs			
RAGE-genistein-argpyrimidine			
N:UNK1:H- A:GLU32:OE2	Hydrogen Bond	Conventional Hydrogen Bond	−6.0
N:UNK1:H- B:ALA41:O	Hydrogen Bond	Conventional Hydrogen Bond	
N:UNK1:H- B:CYS38:O	Hydrogen Bond	Conventional Hydrogen Bond	
B:LYS37:NZ- N:UNK1:O	Hydrogen Bond	Conventional Hydrogen Bond	
N:UNK1- A:PRO33	Hydrophobic	Pi-Alkyl	
N:UNK1 - B:LYS37	Hydrophobic	Pi-Alkyl	
RAGE-apigenin-pentosidine			
N:UNK1:H- A:GLN67:OE1	Hydrogen Bond	Conventional Hydrogen Bond	−5.8
N:UNK1:H- B:SER74:OG	Hydrogen Bond	Conventional Hydrogen Bond	
N:UNK1:H - A:LEU64:O	Hydrogen Bond	Conventional Hydrogen Bond	
N:UNK1:H- A:LEU64:O	Hydrogen Bond	Conventional Hydrogen Bond	
N:UNK1:HN- A:VAL78:O	Hydrogen Bond	Conventional Hydrogen Bond	
N:UNK1:C- A:VAL78:O	Hydrogen Bond	Carbon Hydrogen Bond	
A:LEU79:C,O;PRO80:N- N:UNK1	Hydrophobic	Amide-Pi Stacked	
N:UNK1- A:PRO80	Hydrophobic	Pi-Alkyl	
RAGE-phloretin-pentosidine			
N:UNK1:H- N:UNK1:O	Hydrogen Bond	Conventional Hydrogen Bond	−5.0
N:UNK1:H- N:UNK1:O	Hydrogen Bond	Conventional Hydrogen Bond	
N:UNK1:HN- A:THR195:O	Hydrogen Bond	Conventional Hydrogen Bond	
N:UNK1:HN - A:LYS169:O	Hydrogen Bond	Conventional Hydrogen Bond	
A:ALA197:N - N:UNK1:O	Hydrogen Bond	Conventional Hydrogen Bond	
A:ASP201:N- N:UNK1:O	Hydrogen Bond	Conventional Hydrogen Bond	
N:UNK1:C - A:LYS169:O	Hydrogen Bond	Carbon Hydrogen Bond	
N:UNK1:C- N:UNK1:O	Hydrogen Bond	Carbon Hydrogen Bond	
A:PRO196:CA- N:UNK1:O	Hydrogen Bond	Carbon Hydrogen Bond	
B. AGEs-bioactive compound-RAGE			
Argpyrimidine-phloretin-RAGE			
N:LIG1:N - B:GLY68:O	Hydrogen Bond	Conventional Hydrogen Bond	−8.4
N:UNK1:H- N:UNK1:O	Hydrogen Bond	Conventional Hydrogen Bond	
N:UNK1:H- A:SER74:OG	Hydrogen Bond	Conventional Hydrogen Bond	
N:UNK1:H- B:ASP73:O	Hydrogen Bond	Conventional Hydrogen Bond	
A:GLN67:NE2- N:UNK1:O	Hydrogen Bond	Conventional Hydrogen Bond	
A:SER74:OG- N:UNK1:O	Hydrogen Bond	Conventional Hydrogen Bond	
B:SER74:OG- N:LIG1:O	Hydrogen Bond	Conventional Hydrogen Bond	
A:ASP73:OD2- N:UNK1	Electrostatic	Pi-Anion	
N:LIG1- N:UNK1	Hydrophobic	Pi-Pi Stacked	
N:LIG1- N:UNK1	Hydrophobic	Pi-Pi Stacked	
N:UNK1- N:LIG1:C	Hydrophobic	Pi-Alkyl	
N:UNK1- N:LIG1:C	Hydrophobic	Pi-Alkyl	
Pentosidine-apigenin-RAGE			
N:LIG1:HO- N:LIG1:O	Hydrogen Bond	Conventional Hydrogen Bond	−8.5

Point interaction	Chemistry bond	Type	Binding affinity (kcal/mol)
N:UNK1:H- A:GLN119:OE1	Hydrogen Bond	Conventional Hydrogen Bond	
N:UNK1:H- A:ILE120:O	Hydrogen Bond	Conventional Hydrogen Bond	
B:LYS43:N- N:UNK1:O	Hydrogen Bond	Conventional Hydrogen Bond	
B:LYS43:N- N:UNK1:O	Hydrogen Bond	Conventional Hydrogen Bond	
B:LYS44:N- N:UNK1:O	Hydrogen Bond	Conventional Hydrogen Bond	
N:LIG1:H - N:UNK1:O	Hydrogen Bond	Carbon Hydrogen Bond	
N:LIG1- N:UNK1	Hydrophobic	Pi-Pi T-shaped	
N:UNK1 - B:LYS43	Hydrophobic	Pi-Alkyl	
N:UNK1- B:LYS44	Hydrophobic	Pi-Alkyl	
N:UNK1- B:LYS44	Hydrophobic	Pi-Alkyl	
Pentosidine-genistein-RAGE			
N:LIG1:N- A:LYS169:O	Hydrogen Bond	Conventional Hydrogen Bond	−8.4
N:LIG1:HO- N:UNK1:O	Hydrogen Bond	Conventional Hydrogen Bond	
N:LIG1:HO- A:LYS162:O	Hydrogen Bond	Conventional Hydrogen Bond	
N:LIG1:HO- A:PRO163:O	Hydrogen Bond	Conventional Hydrogen Bond	
N:LIG1:H- A:ASP160:OD2	Hydrogen Bond	Carbon Hydrogen Bond	
N:UNK1:H - N:LIG1:O	Hydrogen Bond	Carbon Hydrogen Bond	
N:LIG1:O- N:UNK1	Hydrogen Bond	Pi-Donor Hydrogen Bond	
N:LIG1- N:UNK1	Hydrophobic	Pi-Pi Stacked	
N:LIG1- A:LEU159	Hydrophobic	Pi-Alkyl	

RAGE-apigenin-argpyrimidine, it was observed that RAGE blocks the binding of naringenin, kaempferol, and apigenin to argpyrimidine, which should bind to RAGE-AGEs. However, argpyrimidine still binds to the RAGE domain, specifically the C1 domain with different chains. On the other hand, the docking of RAGE-genistein-argpyrimidine and RAGE-phloretin-argpyrimidine reveals that RAGE can hinder the binding of genistein and phloretin to argpyrimidine, causing it to translocate from the C1 domain to the V domain. The translocation of argpyrimidine from the C1 domain to the V domain upon binding to genistein and phloretin indicates potentially different biological activities compared to its interaction with RAGE alone. Investigating these alternative binding sites could reveal novel therapeutic avenues [49].

Meanwhile, the docking of RAGE-phloretin-pentosidine and RAGE-apigenin-pentosidine indicates that RAGE can block the binding of phloretin and apigenin while interacting with pentosidine. When tomato compounds and AGEs bind to RAGE, they compete to interact with the RAGE domain. In this study, naringenin, kaempferol, apigenin, genistein, and phloretin successfully interacted with RAGE and displaced the position of AGEs (Fig. S3 and Table S4). The V domain of RAGE serves as a ligand-binding domain, and the two C domains operate as transmembranes. RAGE interacts with AGEs like argpyrimidine and pentosidine, contributing significantly to the problems of DM. Due to an increase in oxidative stress, the production and secretion of pro-inflammatory cytokines, and their binding to RAGE, these ligands cause cellular signal transduction failure [19,45].

The docking results reveal that in the cases of argpyrimidine-naringenin-RAGE, pentosidine-phloretin-RAGE, pentosidine-kaempferol-RAGE, and pentosidine-genistein-RAGE, tomato compounds have a higher affinity for RAGE compared to AGEs, indicating their ability to outcompete AGEs for binding to RAGE (Fig. 3). On the other hand, the docking results of pentosidine-naringenin-RAGE, argpyrimidine-phloretin-RAGE, argpyrimidine-apigenin-RAGE, and pentosidine-apigenin-RAGE show that tomato compounds intervene in the RAGE-AGEs interaction by interacting with AGEs and inducing conformational changes in

AGEs (Fig. S4 and Table S5). These findings suggest that apigenin, genistein, kaempferol, naringenin, and phloretin have the potential to function as competitive inhibitors of AGEs and RAGE interactions, thereby interfering with cellular mechanisms and signal transduction [45]. Furthermore, natural compounds such as polyphenols, polysaccharides, flavonoids, and other natural products have been shown to inhibit AGE formation, which can contribute to lowering blood glucose levels and protecting protein structures [50].

The 5 compounds (genistein, kaempferol, apigenin, naringenin, and phloretin) showed higher root-mean-squared-deviation (RMSD) values compared to the control compound. This indicates that the molecular structures of all compounds during MD simulation showed more fluctuations or were more different from the RAGE structure compared to the control. The ligand movements for all compounds were relatively stable during the MD simulations (Fig. 3).

The stability of their movements indicates that all compounds did not experience significant movements or large fluctuations in their positions during the simulation. The RMSD all shows that genistein, apigenin and naringenin showed higher movement of the protein structure towards side chain flexibility compared to the control compound and phloretin, but at the end of the simulation the genistein, apigenin and naringenin compounds decreased while the control compound increased. This is also related to the number of hydrogen bonds, because the genistein compound at the end of the simulation has more hydrogen bonds than argpyrimidine. RMSD is used to identify the structural stability of the protein-ligand complex [51]. Although the RMSD values were higher for these 5 compounds, this may indicate normal structural variation during MD simulations and not poor stability [52].

■ CONCLUSION

Tomatoes contain genistein and have high antioxidant and antidiabetic properties. Genistein also has promising potential as a therapeutic agent due to its good drug-likeness, moderate to high distribution, and ability to compete with AGEs for RAGE binding.

■ ACKNOWLEDGMENTS

This research was supported by *Hibah Penguatan Ekosistem Guru Besar*, Universitas Brawijaya, Indonesia, grand number 1759.1.14/UN10.C20/2023, and *Hibah Guru Besar* FMIPA, Universitas Brawijaya, Indonesia, grand number 4158.12/UN10.F09/PN/2023. We also thanked all SMONAGENES Research Center members, Universitas Brawijaya, for the discussions.

■ CONFLICT OF INTEREST

The authors declare no conflict of interest.

■ AUTHOR CONTRIBUTIONS

Sekararum Narwasthu contributes to conceptualization, methodology, data collection, sample analysis, validation, data curation, writing – the initial draft. Muhamad Fahmi contributes to methodology, student supervision, writing – revisions, and project management. Titin Andri Wihastuti contributes to methodology, student supervision, writing – revisions. Nia Kurnianingsih contributes to methodology, student supervision, writing – revisions. Fatchiyah contributes to conceptualization, methodology, student supervision, project leadership; project management; and funding acquisition.

■ REFERENCES

[1] Bestari, I.L., 2020, Characteristics of patients with type 2 diabetes mellitus at Surabaya haji general hospital, *Indones. J. Public Health*, 15 (3), 286–294.

[2] Magliano, D.J., Boyko, E.J., and IDF Diabetes Atlas 10th Edition Scientific Committee, 2021, *IDF Diabetes Atlas*, International Diabetes Federation, Brussels, Belgium.

[3] Ratnasari, I., Ngadiarti, I., and Fauziyah, L., 2022, Application of diabetes self-management education and support in outpatients with type II DM, *Media Gizi Indonesia*, 17 (1), 43–50.

[4] Sunday, H.G., Sadia, A.H., and Ojo, O.G., 2022, Mechanisms of diabetes mellitus progression: A review, *J. Diabetic Nephropathy Diabetes Manage.*, 1 (1), 1–5.

[5] Wu, Y., Fu, R., Lei, C., Deng, Y., Lou, W., Wang, L.,

Zheng, Y., Deng, X., Yang, S., Wang, M., Zhai, Z., Zhu, Y., Xiang, D., Hu, J., Dai, Z., and Gao, J., 2021, Estimates of type 2 diabetes mellitus burden attributable to particulate matter pollution and its 30-year change patterns: A systematic analysis of data from the global burden of disease study 2019, *Front. Endocrinol.*, 12, 689079.

[6] Bongarzone, S., Savickas, V., Luzi, F., and Gee, A.D., 2017, Targeting the receptor for advanced glycation endproducts (RAGE): A medicinal chemistry perspective, *J. Med. Chem.*, 60 (17), 7213–7232.

[7] Perrone, A., Giovino, A., Benny, J., and Martinelli, F., 2020, Advanced glycation end products (AGEs): Biochemistry, signaling, analytical methods, and epigenetic effects, *Oxid. Med. Cell. Longevity*, 2020, 3818196.

[8] Xu, K., Zhang, L., Yu, N., Ren, Z., Wang, T., Zhang, Y., Zhao, X., and Yu, T., 2023, Effects of advanced glycation end products (AGEs) on the differentiation potential of primary stem cells: A systematic review, *Stem Cell Res. Ther.*, 14 (1), 74.

[9] Prasad, C., Davis, K.E., Imrhan, V., Juma, S., and Vijayagopal, P., 2019, Advanced glycation end products and risks for chronic diseases: Intervening through lifestyle modification, *Am. J. Lifestyle. Med.*, 13 (4), 384–404.

[10] Oshitari, T., 2023, Advanced glycation end-products and diabetic neuropathy of the retina, *Int. J. Mol. Sci.*, 24 (3), 2927.

[11] Wong, C.Y., Leong, K.H., He, X., Zheng, F., Sun, J., Wang, Z., Heh, C.H., and Kong, K.W., 2022, Phytochemicals of six selected herbal plants and their inhibitory activities towards free radicals and glycation, *Food Biosci.*, 46, 101557.

[12] Kumar, M., Tomar, M., Bhuyan, D.J., Punia, S., Grasso, S., Sá, A.G.A., Carciofi, B.A.M., Arrutia, F., Changan, S., Radha, R., Singh, S., Dhumal, S., Senapathy, M., Satankar, V., Anitha, T., Sharma, A., Pandiselvam, R., Amarowicz, R., and Mekhemar, M., 2021, Tomato (*Solanum lycopersicum* L.) seed: A review on bioactives and biomedical activities, *Biomed. Pharmacother.*, 142, 112018.

[13] Rowaiye, A.B., Oli, A.N., Onuh, O.A., Emeter, N.W., Bur, D., Obideyi, O.A., Dayisi, O.C., Akpa, J.N., Birah, L., Omaka, E.E., Iseghohi, F.O., Otitoju, A.P., Uzor, P.F., and Okoyeh, J.N., 2022, Rhamnetin is a better inhibitor of SARS-CoV-2 2'-O-methyltransferase than dolutegravir: A computational prediction, *Afr. J. Infect. Dis.*, 16 (2), 80–96.

[14] Kirtishanti, A., Siswandono, S., Hardjono, S., and Kesuma, D., 2020, Molecular docking of benzoylurea derivatives as potential anti-breast cancer agent and its ADMET profiles, *J. Global Pharma Technol.*, 12 (6), 726–735.

[15] Abdullah, M.A., Al Dajah, S., Abu Murad, A., El-Salem, A.M., and Khafajah, A.M., 2019, Extraction, purification, and characterization of lycopene from jordanian vine tomato cultivar, and study of its potential natural antioxidant effect on samen baladi, *Curr. Res. Nutr. Food Sci.*, 7 (2), 532–546.

[16] Bettaiah, A., and Prabhushankar, H.B., 2021, Screening of novel source for genistein by rapid and sensitive UPLC-APCI-TOF mass spectrometry, *Int. J. Food Sci.*, 2021, 5537917.

[17] Fatchiyah, F., Sari, D.R.T., Safitri, A., and Cairns, J.R.K., 2020, Phytochemical compound and nutritional value in black rice from Java Island, Indonesia, *Syst. Rev. Pharm.*, 11 (7), 414–421.

[18] Oresanya, I.O., Sonibare, M.A., Gueye, B., Balogun, F.O., Adebayo, S., Ashafa, A.O.T., and Morlock, G., 2020, Isolation of flavonoids from *Musa acuminata* Colla (Simili radjah, ABB) and the *in vitro* inhibitory effects of its leaf and fruit fractions on free radicals, acetylcholinesterase, 15-lipoxygenase, and carbohydrate hydrolyzing enzymes, *J. Food Biochem.*, 44 (3), e13137.

[19] Agustin, A.T., Safitri, A., and Fatchiyah, F., 2021, Java red rice (*Oryza sativa* L.) nutritional value and anthocyanin profiles and its potential role as antioxidant and anti-diabetic, *Indones. J. Chem*, 21 (4), 968–978.

[20] Safitri, A., Roosdiana, A., Kurnianingsih, N., Fatchiyah, F., Mayasari, E., and Rachmawati, R., 2022, Microencapsulation of *Ruellia tuberosa* L. aqueous root extracts using chitosan-sodium

tripolyphosphate and their *in vitro* biological activities, *Scientifica*, 2022, 9522463.

[21] Fatchiyah, F., Safitri, A., Palis, C.N., Sari, D.R.T., Suyanto, E., Fajriani, S., Kurnianingsih, N., Nugraha, Y., Sitaresmi, T., Kusbiantoro, B., and Ketudat-Cairns, J.R., 2023, Bioactive compound profile and their biological activities of endogenous black rice from Java and East Nusa Tenggara, *CyTA - J. Food*, 21 (1), 159–170.

[22] Agustin, A.T., Safitri, A., and Fatchiyah, F., 2020, An *in silico* approach reveals the potential function of cyanidin-3-*O*-glucoside of red rice in inhibiting the advanced glycation end products (AGES)-receptor (RAGE) signaling pathway, *Acta Inform. Med.*, 28 (3), 170–179.

[23] Grahadi, R., Fatchiyah, F., and Kurniawan, N., 2022, Virtual prediction of potential immunogenic epitope of candoxin protein from Malayan krait (*Bungarus candidus*) venom, *J. Pharm. Pharmacogn. Res.*, 10 (6), 1046–1057.

[24] Dallakyan, S., and Olson, A.J., 2015, "Small-Molecule Library Screening by Docking with PyRx" in *Chemical Biology: Methods and Protocols*, Eds. Hempel, J.E., Williams, C.H., and Hong, C.C., Springer, New York, US, 243–250.

[25] Trott, O., and Olson, A.J., 2010, AutoDock Vina: Improving the speed and accuracy of docking with a new scoring function, efficient optimization, and multithreading, *J. Comput. Chem.*, 31 (2), 455–461.

[26] Haque, A., Baig, G.A., Alshawli, A.S., Sait, K.H.W., Hafeez, B.B., Tripathi, M.K., Alghamdi, B.S., Mohammed Ali, H.S.H., and Rasool, M., 2022, Interaction Analysis of MRP1 with anticancer drugs used in ovarian cancer: *In silico* approach, *Life*, 12 (3), 383.

[27] Yuan, S., Chan, H.C.S., and Hu, Z., 2017, Using PyMOL as a platform for computational drug design, *WIREs Comput. Mol. Sci.*, 7 (2), e1298.

[28] Wargasetia, T.L., Ratnawati, H., Widodo, N., and Widyananda, M.H., 2023, Antioxidant and anti-inflammatory activity of sea cucumber (*Holothuria scabra*) active compounds against KEAP1 and iNOS protein, *Bioinf. Biol. Insights*, 17, 11779322221149613.

[29] Kurnianingsih, N., Harbiyanti, N.T., Prakosa, A.G., Ratnawati, R., and Fatchiyah, F., 2022, Materials in life sciences *in silico* study of the 5-hydroxytryptamine-2C receptor antagonist activity of anthocyanins as antidepressant therapy, *J. Mater. Life Sci.*, 2 (1), 88–95.

[30] Sampat, G., Suryawanshi, S.S., Palled, M.S., Patil, A.S., Khanal, P., and Salokhe, A.S., 2022, Drug likeness screening and evaluation of physicochemical properties of selected medicinal agents by computer aided drug design tools, *Adv. Pharmacol. Pharm.*, 10 (4), 234–246.

[31] Padmi, H., Kharisma, V.D., Ansori, A.N.M., Sibero, M.T., Widyananda, M.H., Ullah, M.E., Gumenyuk, O., Chylichcova, S., Bratishko, N., Prasedya, E.S., Sucipto, T.H., and Rahadian, Z., 2022, Macroalgae bioactive compounds for the potential antiviral of SARS-CoV-2: An *in silico* study, *J. Pure Appl. Microbiol.*, 16 (2), 1018–1027.

[32] Ivanović, V., Rančić, M., Arsić, B., and Pavlović, A., 2020, Lipinski's rule of five, famous extensions and famous exceptions, *Chem. Naissensis*, 3 (1), 171–177.

[33] Adianingsih, O.R., Khasanah, U., Anandhy, K.D., and Yurina, V., 2022, *In silico* ADME-T and molecular docking study of phytoconstituents from *Tithonia diversifolia* (Hemsl.) A. Gray on various targets of diabetic nephropathy, *J. Pharm. Pharmacogn. Res.*, 10 (4), 571–594.

[34] Izatunnafis, I., Murti, Y.B., and Sudarmanto, B.S.A., 2023, In silico Pharmacokinetic and toxicity prediction of compounds from *Andrographis paniculata* (Burm.f.) Nees., *J. Food. Pharm. Sci.*, 11 (2), 830–838.

[35] Zackria, A.A., Pattabiraman, R., Murthy, T.P.K., Kumar, S.B., Mathew, B.B., and Biju, V.G., 2022, Computational screening of natural compounds from *Salvia plebeia* R. Br. for inhibition of SARS-CoV-2 main protease, *Vegetos*, 35 (2), 345–359.

[36] Okafor, S.N., Angsantikul, P., and Ahmed, H., 2022,

Discovery of novel HIV protease inhibitors using modern computational techniques, *Int. J. Mol. Sci.*, 23 (20), 12149.

[37] Elshamaa, S.M., Taha, N.M., Lebda, M.A., Hashem, A.E., and Elfeky, M.S., 2022, Zinc oxide nanoparticles alleviated hepatic oxidative stress induced by cadmium chloride toxicity in rats, *Alexandria J. Vet. Sci.*, 73 (1), 1–7.

[38] van Sloun, B., Goossens, G.H., Erdos, B., Lenz, M., van Riel, N., and Arts, I.C.W., 2020, The impact of amino acids on postprandial glucose and insulin kinetics in humans: A quantitative overview, *Nutrients*, 12 (10), 3211.

[39] Vangipurapu, J., Stancáková, A., Smith, U., Kuusisto, J., and Laakso, M., 2019, Nine amino acids are associated with decreased insulin secretion and elevated glucose levels in a 7.4-year follow-up study of 5,181 Finnish men, *Diabetes*, 68 (6), 1353–1358.

[40] Ningsih, I.Y., Wardhani, L.K., Nuryuanda, A.R.E., Puspitasari, E., and Hidayat, M.A., 2022, Genistein content and tyrosinase inhibitory activity of edamame (Glycine max) extracts, *J. Trop. Pharm. Chem.*, 6 (2), 92–100.

[41] Wijayanti, E.D., Safitri, A., Siswanto, D., and Fatchiyah, F., 2023, Indonesian purple rice ferulic acid as a candidate for anti-aging through the inhibition of collagenase and tyrosinase activities, *Indones. J. Chem.*, 23 (2), 475–488.

[42] Telagari, M., and Hullatti, K., 2015, *In-vitro* α-amylase and α-glucosidase inhibitory activity of *Adiantum caudatum* Linn. and *Celosia argentea* Linn. extracts and fractions, *Indian J. Pharmacol.*, 47 (4), 425–429.

[43] Srivalli, R., Kumari, A., Maheswari, U., Prabhakar, N., and Suneetha, J., 2013, *In vitro* studies on alpha amylase and alpha glucosidase inhibitory activities of selected plant extracts, *Int. J. Curr. Res.*, 8 (12), 42739–42742.

[44] Guedes, I.A., de Magalhães, C.S., and Dardenne, L.E., 2014, Receptor-ligand molecular docking, *Biophys. Rev.*, 6 (1), 75–87.

[45] Fatchiyah, F., Hardiyanti, F., and Widodo, N., 2015, Selective inhibition on RAGE-binding AGEs required by bioactive peptide alpha-S2 case in protein from goat Ethawah breed milk: Study of biological modeling, *Acta Inform. Med.*, 23 (2), 90–96.

[46] Friedman, R., 2022, Computational studies of protein–drug binding affinity changes upon mutations in the drug target, *WIREs Comput. Mol. Sci.*, 12 (1), e1563.

[47] Moysa, A., Steczkiewicz, K., Niedzialek, D., Hammerschmid, D., Zhukova, L., Sobott, F., and Dadlez, M., 2021, A model of full-length RAGE in complex with S100B, *Structure*, 29 (9), 989–1002.e6.

[48] Faisal, M.A., Oktaviyanti, I.K., Sujuti, H., and Rudijanto, A., 2020, Virtual screening of the active components of *Garcinia mangostana* Linn. Potentially inhibiting the interaction of advanced glycation end-products and their receptor, *Open Access Maced. J. Med. Sci.*, 8 (A), 921–927.

[49] Patil, R., Das, S., Stanley, A., Yadav, L., Sudhakar, A., and Varma, A.K., 2010, Optimized hydrophobic interactions and hydrogen bonding at the target-ligand interface leads the pathways of drug-designing, *PLoS One*, 5 (8), e12029.

[50] Li, L., Song, Q., Zhang, X., Yan, Y., and Wang, X., 2022, Allicin alleviates diabetes mellitus by inhibiting the formation of advanced glycation end products, *Molecules*, 27 (24), 8793.

[51] Liu, K., Watanabe, E., and Kokubo, H., 2017, Exploring the stability of ligand binding modes to proteins by molecular dynamics simulations, *J. Comput.-Aided Mol. Des.*, 31 (2), 201–211.

[52] Yun, S., and Guy, H.R., 2011, Stability tests on known and misfolded structures with discrete and all atom molecular dynamics simulations, *J. Mol. Graphics Modell.*, 29 (5), 663–675.